Journal of Organometallic Chemistry, 398 (1990) 133–158
Elsevier Sequoia S.A., Lausanne
JOM 21074

Synthesis and structure of osmium and ruthenium complexes containing tetrafluoroethylene and maleic anhydride as ligands

A.K. Burrell, G.R. Clark, C.E.F. Rickard, W.R. Roper * and D.C. Ware

Department of Chemistry, University of Auckland, Private Bag, Auckland (New Zealand)

(Received May 14th, 1990)

Abstract

The d^8 complexes, $M(CO)(L)(PPh_3)_3$ ($M = Ru$, Os; $L = CO$, CNR; $R = p$-tolyl) and $OsCl(NO)(PPh_3)_3$, all form simple 1:1 π-adducts with tetrafluoroethylene and maleic anhydride, with the overall coordination geometry being dependent upon the relative electron-withdrawing properties of the olefin and the relative electron richness of the metal fragment. In all the tetrafluoroethylene complexes of ruthenium examined, the geometry of the complex involves *cis*-triphenylphosphine ligands. The X-ray crystal structure of $Ru(C_2F_4)(CO)_2(PPh_3)_2$ is presented as an example of this structural class. $Ru(C_2F_4)(CO)_2(PPh_3)_2$ crystallises in the monoclinic space group $P2_1/a$ with a cell having dimensions $a = 35.940(2)$, $b = 10.655(7)$, $c = 18.559(6)$ Å and $\beta = 93.21(3)°$, with two crystallographically independent molecules in the asymmetric unit ($Z = 8$). The osmium complexes do not display this strong preference for *cis*-triphenylphosphine ligands and $Os(C_2F_4)(CO)_2(PPh_3)_2$ exists as two separate but interconvertible isomers in solution. One isomer has the same relative geometry as $Ru(C_2F_4)(CO)_2(PPh_3)_2$. The other has *trans*-triphenylphosphine ligands. This temperature-dependent equilibrium has been studied by variable-temperature NMR and has $\Delta H° = -15$ kJ mol^{-1} and $\Delta S° = -60$ J K^{-1} mol^{-1}.

The maleic anhydride complexes also show a variation in geometry from the usual *trans* triphenylphosphine arrangement. The X-ray crystal structure of Os(maleic anhydride)$(CO)_2(PPh_3)_2$ is reported along with the solution structures of other maleic anhydride complexes. Os(maleic anhydride)$(CO)_2(PPh_3)_2$ crystallises in the monoclinic space group $P2_1/c$ with a cell having dimensions $a = 23.667(2)$, $b = 20.306(1)$, $c = 16.147(1)$ Å and $\beta = 93.20(1)°$, with two crystallographically independent molecules in the asymmetric unit ($Z = 8$). The triphenylphosphine ligands are again *cis* but only one lies in the plane of the osmium and the coordinated olefin.

0022-328X/90/$03.50

Introduction

Osmium and ruthenium zero-valent complexes of the type $M(CO)(L)(PPh_3)_3$ and $OsCl(NO)(PPh_3)_3$ (M = Os, Ru; L = CO, CS, CNR, etc.), undergo reactions with a number of unsaturated molecules forming compounds which can be described as simple π-complexes [1–6].

Previous studies of the complexes $M(CO)(L)(PPh_3)_3$ and $OsCl(NO)(PPh_3)_3$ (M = Os, Ru; L = CO, CS, CNR), with electron-withdrawing olefins, have been limited to a number of cyanoolefins [7]. There is also one reported reaction of maleic anhydride with Ru(CN-*p*-tolyl)(CO)$(PPh_3)_3$ [7,8]. The study reported herein has led to complexes with some unexpected geometries and some insight has been gained into the effect of varying the electron-withdrawing ability of the ligand on the preferred metal geometry of the resulting complex.

Results and discussion

$Ru(CO)_2(PPh_3)_3$ reacts with tetrafluoroethylene at room temperature, over a period of an hour, to give the complex $Ru(C_2F_4)(CO)_2(PPh_3)_2$. The compound is a white crystalline solid which is slightly light sensitive. The product has only one major ν(CO) band (1990 cm^{-1}) in the IR spectrum (solution and Nujol mull) (see Table 1). Examination of the NMR data indicated that the complex contained two equivalent *cis* PPh_3 ligands and two equivalent carbonyl groups along with a

Table 1

IR data [a] for C_2F_4 and MA complexes of Ru and Os

Complex	ν(CO) [c]	ν(CF) [c]	Other bands
$Ru(C_2F_4)(CO)_2L_2$	1990	1358, 1090, 1067, 1025, 800	
$Os(C_2F_4)(CO)_2L_2$	1979 (2015, 1948, 1985) [b]	1092, 1063, 1029, 818,	
$Ru(C_2F_4)(CO)(CNR)L_2$	1978	1063, 1018 797	2156 (CN)
$Os(C_2F_4)(CO)(CNR)L_2$	1968	1377, 1090 1056, 1019 820	2160 (CN)
$Os(C_2F_4)(CS)(CO)L_2$	2031	1091, 1067 1022	1302 (CS)
$Os(C_2F_4)Cl(NO)L_2$		1094, 1087 1035, 824	1715 (NO)
$Ru(MA)(CO)_2L_2$	2026, 2017(sss), 1968, 1959(sss), 1797, 1732		1229m (MA)
$Os(MA)(CO)_2L_2$	2000, 1930, 1801, 1733		1229m, (MA)
$Os(MA)Cl(NO)L_2$	1808, 1738		1780 (NO) 1221m (MA)

[a] Recorded as Nujol mulls and reported in cm^{-1}, sss = multiple bands attributed to solid-state splitting, L = PPh_3, R = *p*-tolyl. [b] CH_2Cl_2 solution. [c] All bands strong unless stated otherwise.

η^2-tetrafluoroethylene ligand. The structure was, therefore, assigned as below (Eq. 1).

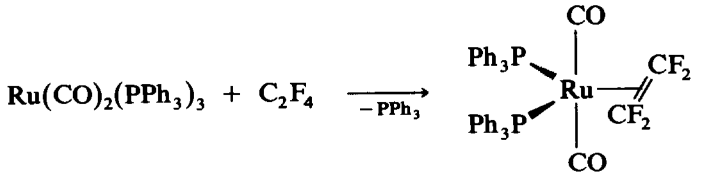

(1)

The same complex was generated by the thermal reaction between C_2F_4 and $Ru(CO)_3(PPh_3)_2$ or $Ru(C_2H_4)(CO)_2(PPh_3)_2$. The reaction of $Ru(CO)_2(PPh_3)_3$ with tetrafluoroethylene had previously been reported [7]. The product described in ref. 7, was assigned the structure of a complex containing a ruthenacyclopentane ring (Eq. 2). The reaction was reported as having been carried out using dichloromethane as the solvent. This is unfortunate since $Ru(CO)_2(PPh_3)_3$ is known to be reactive towards halogenated solvents [6]. The only properties reported for the proposed product were the molecular weight; ν(CO) (2057s, 1999s); and microanalytical data. The analytical data were correct only when the presence of one dichloromethane of solvation was assumed. Other means of confirmation for the formulation, particu-

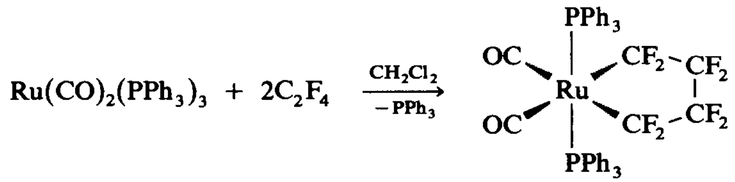

(2)

larly NMR data, were not presented. The compound isolated is more likely to be $RuCl(CF_2CF_2H)(CO)_2(PPh_3)_2$. All of the data (including the reported analytical data and molecular weight) are consistent with this formulation. The synthesis and full characterisation of $RuCl(CF_2CF_2H)(CO)_2(PPh_3)_2$ has been described [9].

As the final confirmation of the structure of $Ru(C_2F_4)(CO)_2(PPh_3)_2$, an X-ray crystal structure determination was carried out.

Description of X-ray structure of $Ru(C_2F_4)(CO)_2(PPh_3)_2$

$Ru(C_2F_4)(CO)_2(PPh_3)_2$ crystallises in the space group $P2_1/a$ with two crystallographically independent molecules in each asymmetric unit. All the heavy atoms (excluding carbon) were refined using the anisotropic model. Many data were weak due to the packing of the two independent molecules, $x' \approx x$ and $z' \approx 1/2 + z$, as a result, refinement converged to a residual of 0.096. All of the atoms were well defined and the ESD's on all bond lengths and angles were satisfactory. The data were collected at room temperature, so the thermal motion of the fluorine atoms resulted in slightly high thermal parameters for these atoms.

The structure (Fig. 1) is that of a distorted trigonal bipyramid. The two carbonyl ligands occupy both of the axial sites, with the *cis* triphenylphosphine ligands and the tetrafluoroethylene in the equatorial plane. The metal–carbon bond lengths involving the tetrafluoroethylene ligands are normal (see Tables 2 and 3). The carbon–carbon bond length of the tetrafluoroethylene ligand has increased upon coordination, and at 1.46 Å, is normal for a coordinated C_2F_4 (Table 4).

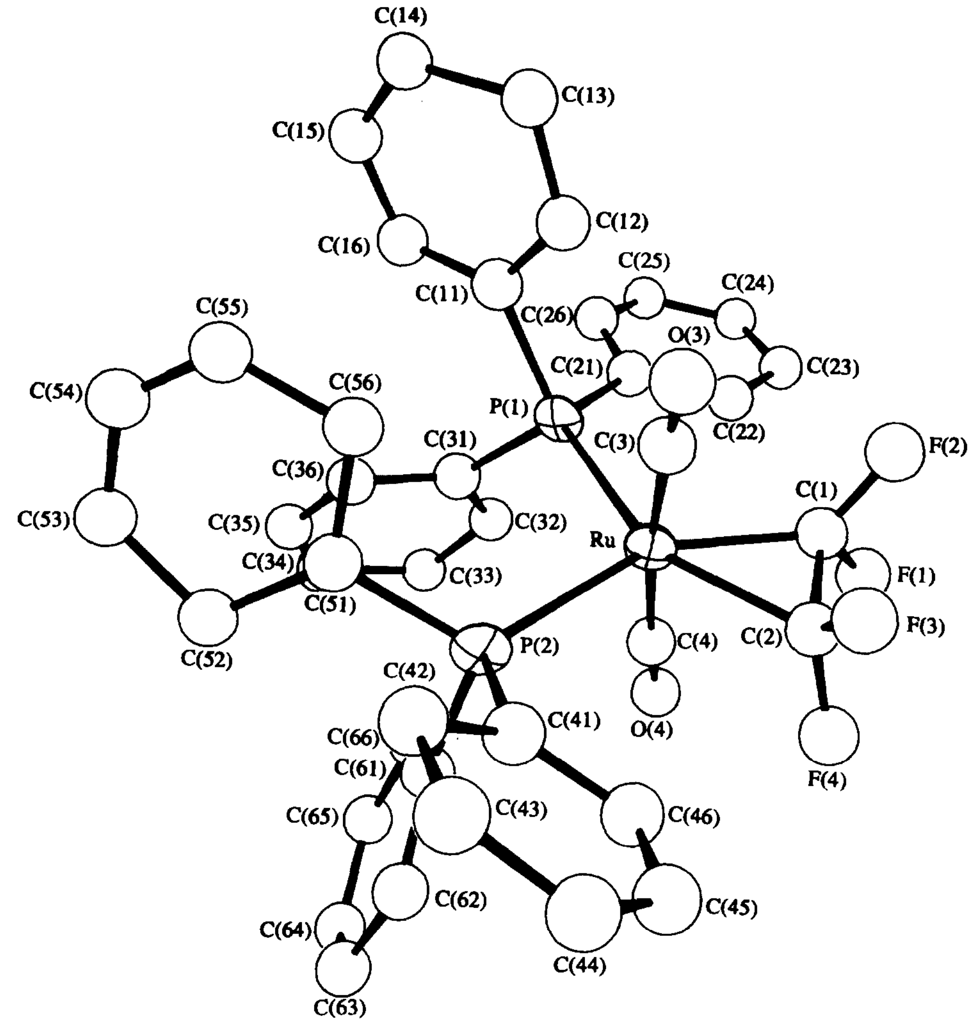

Fig. 1. The molecular geometry (molecule 1) and atomic numbering scheme for $Ru(C_2F_4)(CO)_2(PPh_3)_2$.

Synthesis and geometry of $Os(C_2F_4)(CO)_2(PPh_3)_2$

Prior to this work only one tetrafluoroethylene complex of osmium had been reported [8]. This involved the thermal addition of C_2F_4 to $Os(CO)_3[P(OMe)_3]_2$ resulting in displacement of one of the carbonyl ligands and isolation of $Os(C_2F_4)(CO)_2[P(OMe)_3]_2$. This adduct has the same geometry as $Ru(C_2F_4)(CO)_2$-

Table 2

Selected bond lengths (Å) (Av.) for $Ru(C_2F_4)C(O)_2(PPh_3)_2$

Ru–P1	2.391(8)	Ru–C2	2.11(3)	Cl–C2	1.46(4)
Ru–P2	2.406(7)	Ru–C3	1.94(4)	Cl–F(1, 2)	1.37(4) [a]
Ru–Cl	2.06(3)	Ru–C4	1.90(4)	C2–F(3, 4)	1.37(4) [b]

[a] Average of F1 and F2. [b] Average of F3 and F4.

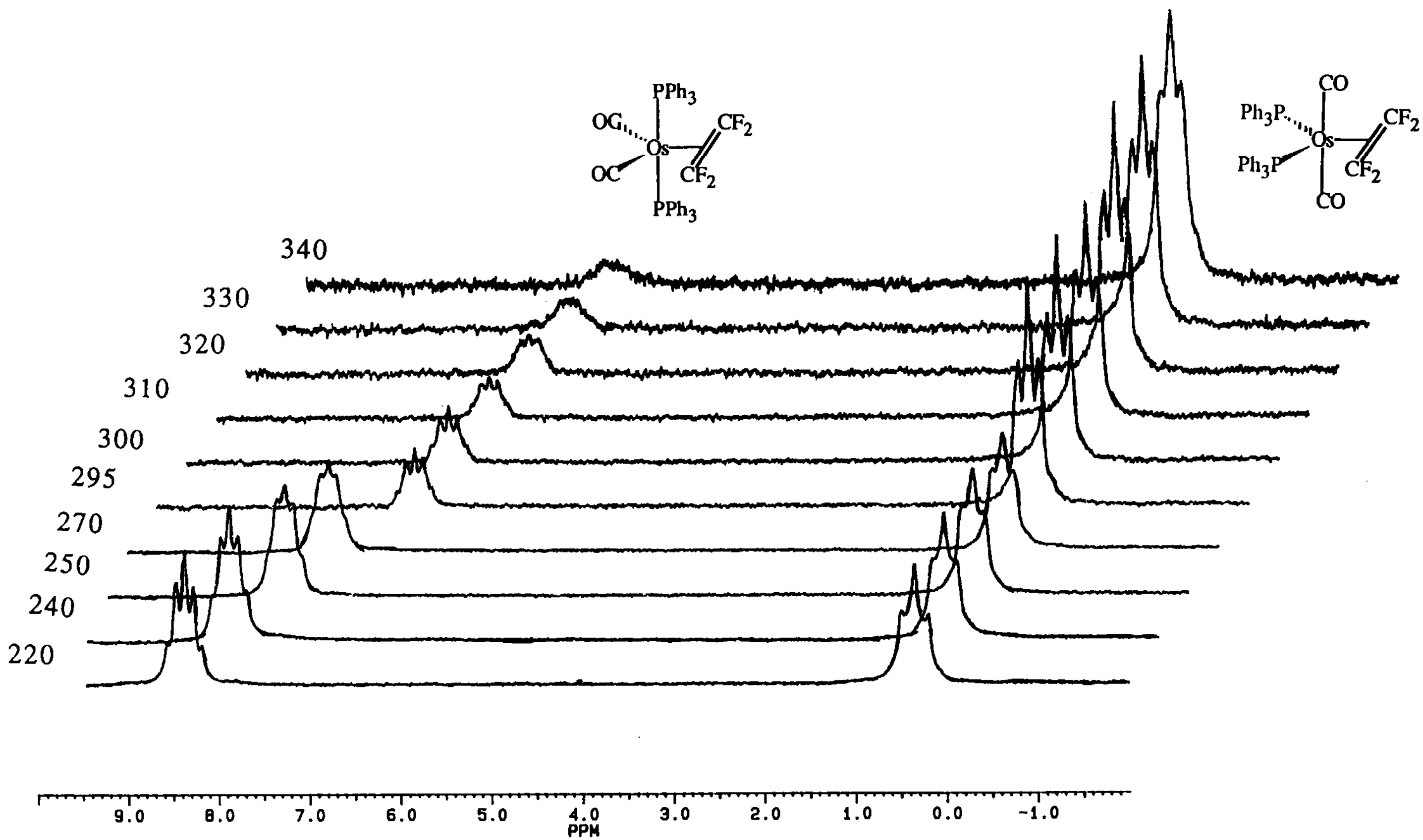

Fig. 2. ^{31}P NMR spectra of $Os(C_2F_4)(CO)(PPh_3)_2$ at various temperatures (K).

Table 3

Selected bond angles (°) (Av.) for $Ru(C_2F_4)(CO)_2(PPh_3)_2$

P1-Ru-P2	101.4(3)	P2-Ru-C2	110(1)	C2-Ru-C3	84(1)		
P1-Ru-C1	107(1)	P2-Ru-C3	88(1)	C2-Ru-C4	88(1)		
P1-Ru-C2	149(1)	P2-Ru-C4	95(1)	C3-Ru-C4	172(1)		
P1-Ru-C3	95(1)	C1-Ru-C2	40(1)	F1-C1-F2	40.4(6)		
P1-Ru-C4	87(1)	C1-Ru-C3	88(1)	F3-C2-F4	42.1(6)		
P2-Ru-C1	150(1)	C1-Ru-C4	87(1)				

$(PPh_3)_2$ with the carbonyl groups mutually *trans* and with *cis* trimethylphosphites in the equatorial plane with the C_2F_4 ligand.

In a reaction analogous to the addition of tetrafluoroethylene to $Ru(CO)_2(PPh_3)_3$, $Os(CO)_2(PPh_3)_3$ was heated under C_2F_4 (500 kPa at 90 °C) for 12 hours to ensure complete reaction. These more vigorous conditions were required to overcome the kinetic inertness typical of osmium complexes. The resulting complex, $Os(C_2F_4)(CO)_2(PPh_3)_2$ (Eq. 3), is a white crystalline solid which does not show the light

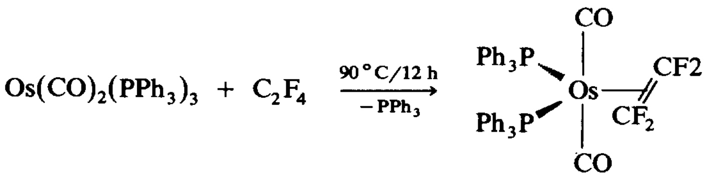

(3)

sensitivity of the ruthenium analogue. The IR spectrum, taken as a Nujol mull, showed a single ν(CO), however, when recorded in dichloromethane, three carbonyl stretches were evident. Multinuclear NMR spectra confirmed the presence of two isomers in solution.

The ^{13}C NMR spectrum also showed signals assignable to two species in solution (Table 5). Analysis of the spectrum confirmed that both isomers have geometries which resulted in equivalent triphenylphosphine ligands. The major species has a simple doublet coupling pattern for the *ipso* carbon of the triphenylphosphine

Table 4

Comparison of bond lengths for coordinated C_2F_4

Complex	M-C (Å)(Av.)	C-C (Å)	Ref.
$Ir(CF_3)(C_2F_4)(CO)(PPh_3)_2$	2.12(4)	1.59(5)	9
$Ru(C_2F_4)(CO)_2(PPh_3)_2$	2.09(3)	1.46(4)	[a]
$Ru(C_2F_4)Cl(NO)(PPh_3)(CH_2PPh_3)$	2.05(2)	1.42(3)	[b]
$Fe(C_2F_4)(CO)_4$	1.99(1)	1.53(2)	10
$RhCl(C_2F_4)(PPh_3)_2$	2.00(8)	1.41(3)	11
$(acac)Rh(C_2F_4)(C_2H_4)$	2.01(1)	1.40(2)	12
$[FRh(C_2F_4)(C_2H_4)]_4$	1.97(4)	1.430(7)	13
$CpRh(C_2F_4)(C_2H_4)$	2.024(2)	1.405(7)	14
$Pt(C_2F_4)(AsPh_3)_2$	2.015(1)	1.45(2)	15
$Pt(C_2F_4)(C_2H_4)_2$	1.97(3)	1.44(4)	16
$Pt(C_2F_4)(C_2H_4)(PCy_3)$	2.03(1)	1.45(2)	17

[a] This work. [b] A.K. Burrell, C.E.F. Rickard, W.R. Roper and A.H. Wright, unpublished.

Table 5

^{13}C NMR data [a] for C_2F_4 complexes of Ru and Os

Complex	PPh$_3$ ipso	^1J(CP)	ortho	^2J(CP)	meta	^3J(CP)	para	^4J(CP)	C_2F_4 δ	^1J(CF)	^1J(CF′)	^2J(CP)	CO (δ)	CN (δ)	CH_3 (δ)	other (δ)
$Ru(C_2F_4)(CO)(CNR)L_2$	137.3d	34.4	133.4d	12.3	128.0d	9.2	129.2d	1.1	120.9ddd	399.1	399.1	63.6	199.3m	202.1m	21.3s	139.0s 125.9s 129.5s 128.3s
$Ru(C_2F_4)(CO)_2L_2$	135.9d	36.8	133.1d	12.3	128.3d	9.7	129.8d	1.3	119.0ddd	344.4		53.6	199.3m			
$Os(C_2F_4)(CO)_2L_2$ [b]	135.9d	46.9	133.2d	12.0	128.2d	10.1	130.0s		100.0ddd	331.9		38.7	185.1m			
$Os(C_2F_4)(CO)_2L_2$ [c]	135.5t	36.5	134.5t	5.5	128.0t	5.0	130.4t		101.0t	324.3			186.5m			
$Os(C_2F_4)(CO)(CNR)L_2$	137.3d	44.2	133.4d	11.7	127.9d	9.6	129.3s		101.6ddd	330.3	330.0	49.2	147.5m	187.2m	21.3s	139.1s 129.4s 124.8s 125.1s
$Os(C_2F_4)Cl(NO)L_2$	136.3t	31.4	128.1t	5.3	134.7t	4.7	130.7s		118.7tm 101.5tm	321.2 315.1						

[a] Recorded in $CDCl_3$ at 25 °C and reported in ppm with coupling constants in Hz, s = singlet, d = doublet, t = triplet, m = multiplet, L = PPh_3, R = *p*-tolyl. [b] *trans*-CO ligands. [c] *cis*-CO ligands.

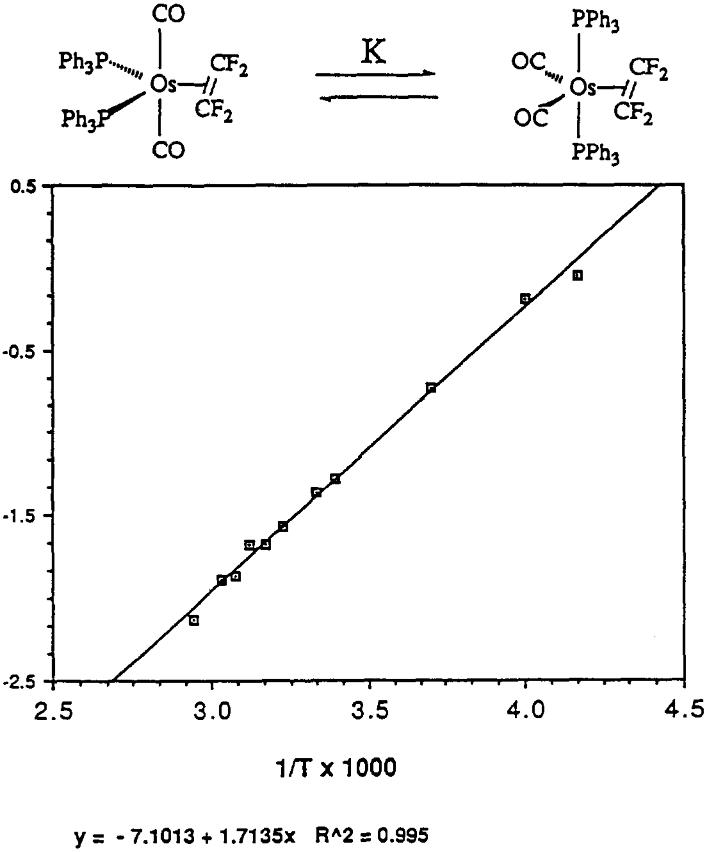

Fig. 3. Van't Hoff plot of the $Os(C_2F_4)(CO)_2(PPh_3)_2$ *cis–trans* equilibrium.

ligand. This isomer is isostructural with $Ru(C_2F_4)(CO)_2(PPh_3)_2$ and retains the same geometry as the crystalline solid.

The second isomer has a triplet pattern for the *ipso* carbons of the PPh_3 ligands. This, then, is the isomer with equivalent *trans* triphenylphosphine ligands (Eq. 4).

The signals for the carbons of the tetrafluoroethylene ligands showed two separate coupling patterns for each of the isomers. The isomer of $Os(C_2F_4)(CO)_2(PPh_3)_2$ with *trans* PPh_3 groups, gave rise to a triplet, resulting from the ^1J(CF) coupling only to the two attached fluorines. There was, however, further coupling evident, but it could not be resolved. The other isomer (with *cis* PPh_3 ligands) had a coupling pattern for the C_2F_4 carbons similar to that seen in $Ru(C_2F_4)(CO)_2(PPh_3)_2$, i.e. a doublet of triplets.

The two isomers of $Os(C_2F_4)(CO)_2(PPh_3)_2$ were found to be present in a temperature-dependent equilibrium in solution (Eq. 4). A series of variable temperature ^{31}P NMR spectra were collected. At all temperature for which spectra could be obtained both isomers appeared as separate signals (Fig. 2) While there was some chemical shift temperature-dependence, the two signals never approached coalescence. The relative amounts of the two isomers of $Os(C_2F_4)(CO)_2(PPh_3)_2$ were assessed by determining the integrals of the two ^{31}P NMR resonances. Using these relative ratios over the range of temperatures recorded, a Van't Hoff plot was calculated (Fig. 3). From this plot $\Delta H°$ (−15 kJ mol^{-1}) and $\Delta S°$ (−60 J K^{-1} mol^{-1}) were calculated. The equilibrium is, therefore, dominated by the entropy

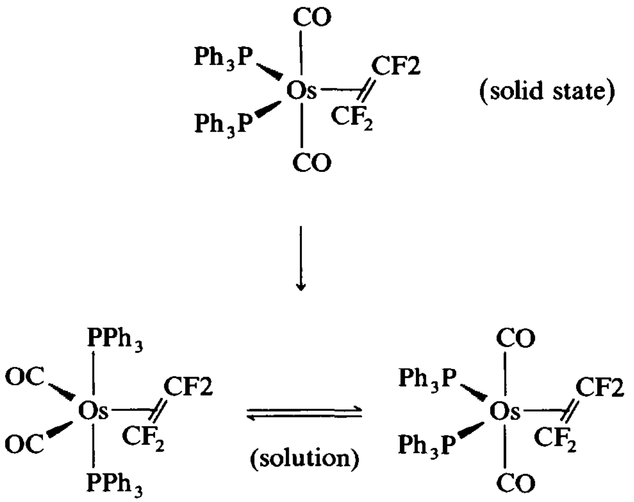

(4)

1 : 3

Table 6

^{1}H, ^{31}P and ^{19}F NMR data [a] for C_2F_4 and maleic anhydride complexes of Ru and Os

Complex	^{31}P δ	$^{2}J(PP)$	^{19}F (δ)	^{1}H Olefinic	$^{3}J(PH)$	$^{3}J(P'H)$
$Ru(C_2F_4)(CO)_2L_2$	31.8m		−110m			
$Ru(C_2F_4)(CNR)(CO)L_2$	34.5m		−108m, −110m			
			−113m, −115m			
$Os(C_2F_4)(CO)_2L_2$ [b]	0.2m		−113m			
$Os(C_2F_4)(CO)_2L_2$ [c]	6.3m		−115m			
$Os(C_2F_4)(CO)(CNR)L_2$	3.5m					
$Os(C_2F_4)(CS)(CO)L_2$ [d]	7.8m					
$Os(C_2F_4)(CS)(CO)L_2$ [e]	2.5m					
$Os(C_2F_4)Cl(NO)L_2$	−1.3m		−113m, −103m			
$Ru(MA)(CO)_2L_2$	33.9d	25.1		3.01m		
	30.0d			1.18m		
$Os(MA)(CO)_2L_2$	−4.2d	19.5		3.04m		
	2.1d			1.74m		
$Os(MA)Cl(NO)L_2$	−8.5s			3.72s		
$Ru(MA)(CO)(CNR)L_2$ (A)	40.2s			3.18d	3.4	
$Ru(MA)(CO)(CNR)L_2$ (B)	39.2d	24.0		3.12dd	4.0	6.1
	34.3d			3.08dd	4.3	6.0
$Ru(MA)(CO)(CNR)L_2$ (C)	33.9d	24.6				
	29.9d					
$Ru(MA)(CO)(CNR)L_2$ (D)	38.5d	359				
	26.3d					

[a] Recorded in $CDCl_3$ at 25 °C and reported in ppm with coupling constants in Hz, s = singlet, d = doublet, t = triplet, m = multiplet, L = PPh_3, R = *p*-tolyl. [b] *trans*-CO ligands. [c] *cis*-CO ligands. [d] CS *cis* to CO. [e] CS *trans* to CO

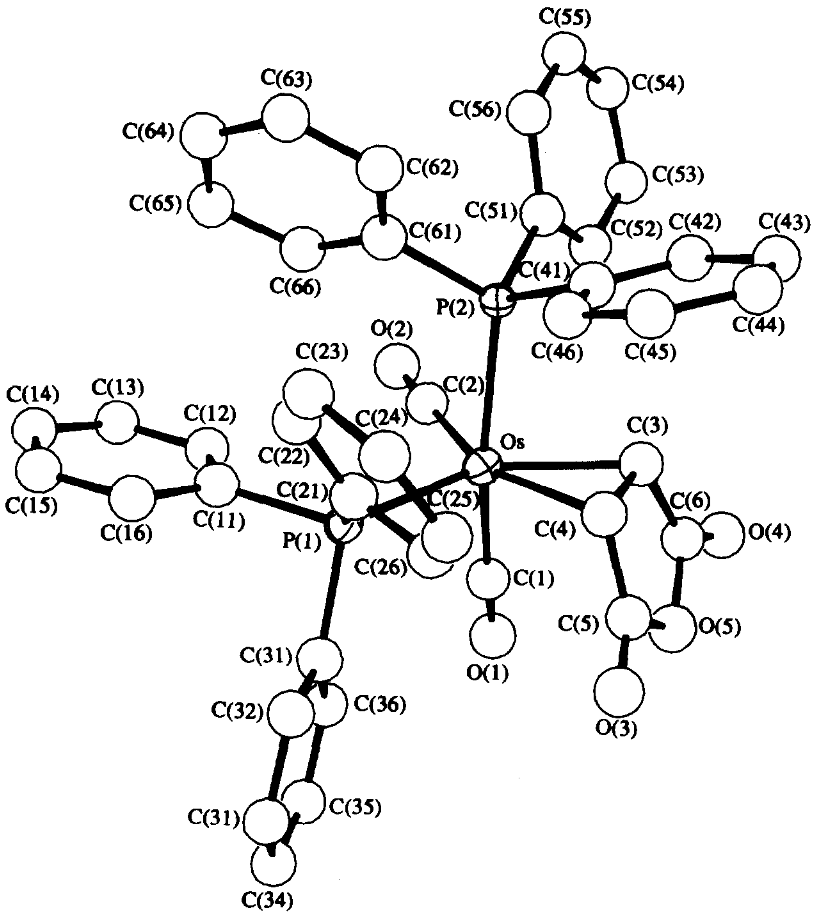

Fig. 4. The molecular geometry (molecule 1) and atomic numbering scheme for $Os(MA)(CO)_2(PPh_3)_2$.

term. It is not immediately apparent why one isomer should be entropy-favoured over the other. These values for $\Delta H°$ and $\Delta S°$ are similar to those found for the Berry rotation in the complex Ru(fumaronitrile)$(CO)_2(PPh_3)_2$ [7]. The only other tetrafluoroethylene complex found to display a similar equilibrium in solution was $Os(C_2F_4)(CS)(CO)(PPh_3)_2$. Unfortunately, owing to the low yields in the synthesis of $Os(C_2F_4)(CS)(CO)(PPh_3)_2$, and contamination of samples by paramagnetic material, this compound was not investigated further.

In contrast to the behaviour of $Os(C_2F_4)(CO)_2(PPh_3)_2$, the ^{31}P NMR spectrum of the analogous ruthenium complex, $Ru(C_2F_4)(CO)_2(PPh_3)_2$, is temperature-independent (Table 6).

The unusual geometry and equilibrium situation encountered for the tetrafluoroethylene adducts of $M(CO)_2(PPh_3)_2$ (M = Ru, Os) have been previously observed for some cyanoolefins [7]. The strong electron-withdrawing nature of these olefins has a direct effect upon the geometry at the metal and to further investigate this effect, several maleic anhydride complexes were made.

Table 7

^{13}C NMR data [a] for maleic anhydride complexes of Ru and Os

Complex	PPh$_3$								Maleic anhydride						CO			CN	
	ipso	^1J(CP)	*ortho*	^2J(CP)	*meta*	^3J(CP)	*para*	^4J(CP)	CH	^3J(CP)	^3J(CP′)	C=O	^2J(CP)	^2J(CP′)	δ	^2J(CP)	^2J(CP′)	δ	^2J(CP)
Ru(MA)(CO)$_2$L$_2$	135.4d	38.2	133.8 [a]		128.6 [b]		130.2d	2.0	23.6dd	2.9	3.0	177.2dd	1.6	2.8	204.0dd	20.1	1.1		
	130.1d	40.1	133.8 [a]		128.6 [b]		131.0d	2.0	38.7dd	19.8	4.9	177.3dd	4.0	3.8	197.5dd	92.1	10.1		
Os(MA)(CO)$_2$L$_2$	135.0d	47.9	128.6d	10.0	134.7d	5.0	130.2d	2.0	27.7dd	5.3	2.9	177.3dd			187.2dd	15.9	5.3		
	130.9d	43.6	133.3d	9.4	[c]		130.9d	2.0	23.4dd	18.6	4.1	176.5dd			180.0dd	87.0	7.8		
Ru(MA)(CO)-(CNR)L$_2$ (A)	136.8m		128.1m		133.5m		129.6m		33.7m			177.4s			164.0t	16.9		203.2t	13.0
Ru(MA)(CO)-(CNR)L$_2$ (B)	129.9t	24.6							37.8dd	16.4	5.2	178.7m			162.8m			206.3d	19.7
									35.0dd	4.1	3.9	176.9m							
Os(MA)Cl-(NO)L$_2$	131.6t	24.4	128.4t	5.2	134.0t	5.0	130.4s		44.7t	13.5									

[a] Recorded in CDCl$_3$ at 25 °C and reported in ppm with coupling constants in Hz, s = singlet, d = doublet, t = triplet, m = multiplet, L = PPh$_3$, R = *p*-tolyl.

Maleic anhydride complexes of $Os(CO)_2(PPh_3)_3$ and $Ru(CO)_2(PPh_3)_3$

When $Ru(CO)_2(PPh_3)_3$ was treated with one equivalent of maleic anhydride an immediate reaction occurred. The product was a colourless crystalline solid which analysed correctly for $Ru(MA)(CO)_2(PPh_3)_2$ (where MA = maleic anhydride). The IR spectrum of $Ru(MA)(CO)_2(PPh_3)_2$ displayed two metal bound carbonyl stretches (2028 and 1965 cm^{-1}). The maleic anhydride ligand was evident by the presence of two strong ν(C=O) stretches at 1796 and 1730 cm^{-1}. The presence of two metal carbonyl stretches in the IR spectrum ruled out a solid state structure similar to that of $Ru(C_2F_4)(CO)_2(PPh_3)_2$. The NMR data indicated that $Ru(MA)(CO)_2(PPh_3)_2$ had a structure which contained two inequivalent *cis* triphenylphosphine ligands (Tables 6 and 7). The structure was therefore assigned as being on of the two possible isomers with *cis* PPh_3 ligands and *cis* carbonyl groups (Eq. 5).

$Ru(CO)_2(PPh_3)_3$ + Maleic Anhydride $\longrightarrow$

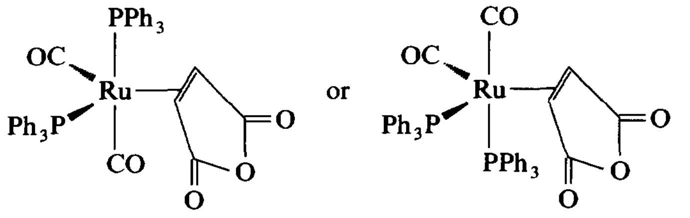

(5)

(A) (B)

Unfortunately, the exact geometry of the complex could not be determined by NMR, with either isomer **A** or **B** being consistent with the data.

The analogous osmium complex could not be made directly from $Os(CO)_2(PPh_3)_3$. The reaction of maleic anhydride with $Os(CO)_2(PPh_3)_3$ was very slow and the product contained significant amounts of an impurity, $Os(O_2)(CO)_2(PPh_3)_2$, along with starting material. In a number of reactions involving the transient species "$Os(CO)_2(PPh_3)_2$", the ethylene complex $Os(C_2H_4)(CO)_2(PPh_3)_2$ has been used as a precursor [6]. This proved to be useful in the formation of $Os(MA)(CO)_2(PPh_3)_2$. The complex $Os(MA)(CO)_2(PPh_3)_2$ has NMR and IR characteristics similar to those of $Ru(MA)(CO)_2(PPh_3)_2$. As with $Ru(MA)(CO)_2(PPh_3)_2$, it was not possible to completely determine the geometry of the maleic anhydride complex by NMR. Therefore, it became necessary to rely upon an X-ray structural determination.

Description of the X-ray structure of $Os(MA)(CO)_2(PPh_3)_2$

$Os(MA)(CO)_2(PPh_3)_2$ crystallised in the space group $P2_1/c$. The asymmetric unit contained two crystallographically independent, but otherwise similar, molecules of $Os(MA)(CO)_2(PPh_3)_2$. The data refined to give $R = 0.0723$ and $R_w =$

Table 8

Selected bond lengths (Å) (Av.) for $Os(MA)(CO)_2(PPh_3)_2$

Os–P1	2.403(6)	Os–C2	1.95(3)	Os–C4	2.19(2)
Os–P2	2.457(7)	Os–C3	2.18(2)	C3–C4	1.43(3)
Os–C1	1.87(3)				

Table 9

Selected bond angles (°) (Av.) for $Os(MA)(CO)_2(PPh_3)_2$

P1–Os–P2	99.3(2)	P2–Os–C1	165.1(9)	C1–Os–C3	92(1)
P1–Os–C1	93.1(6)	P2–Os–C2	85.0(9)	C1–Os–C4	97(1)
P1–Os–C2	105.1(9)	P2–Os–C3	84.5(7)	C2–Os–C3	119(1)
P1–Os–C3	136.4(7)	P2–Os–C4	89.0(9)	C2–Os–C4	157(1)
P1–Os–C4	97.9(6)	C1–Os–C2	84(1)	C3–Os–C4	38.5(9)

0.0760, with all atoms except the phenyl carbons being refined using the anisotropic model. The geometry about the osmium was approximately trigonal bipyramidal with the maleic anhydride, a phosphine and carbonyl occupying the equatorial plane (Fig. 4). The axial positions were occupied by the other carbon monoxide and the remaining phosphine ligand. The important bond lengths and angles are reported in Tables 8 and 9. The osmium–maleic anhydride bond lengths (Os-C3 and Os-C4) were within the expected ranges for maleic anhydride complexes (Table 10). The olefinic bond (C3–C4) was significantly longer than the corresponding distance (1.303 Å) in free maleic anhydride. Again, this distance is within the expected range for coordinated maleic anhydride (Table 10). The maleic anhydride has adopted the conformation in which there is the least steric pressure, with the ring of the maleic anhydride ligand being tilted down over the smaller carbon monoxide ligand. There is probably insufficient room for the maleic anhydride ligand to occupy the other geometry (covering the PPh_3).

$OsCl(NO)(PPh_3)_3$ and electron withdrawing olefins

$OsCl(NO)(PPh_3)_3$ has been reacted with a number of species containing multiple bonds to form π-adducts [28]. These complexes readily lose the olefin in most cases. No reactions of electron-deficient olefins had previously been studied with $OsCl(NO)(PPh_3)_3$. However, the ruthenium analogue had been shown to form a simple π-adduct with tetrafluoroethylene [25]. This complex was reported to readily lose the C_2F_4 ligand in solution.

The addition of tetrafluoroethylene to $OsCl(NO)(PPh_3)_3$ in dry, degassed, ben-

Table 10

Comparison of bond lengths for coordinated maleic anhydride

Complex	M–C (Å)(Av)	C–C (Å)	Ref.
$Os(MA)(CO)_2(PPh_3)_2$	2.19(2)	1.43(3)	[a]
$Ru(MA)(CO)(CNR)(PPh_3)_2$ [b]	2.19(1)	1.45(2)	8
$Co(MA)(P(OMe)_3)_3$	2.033(7)	1.451(1)	19, 20
$W(MA)(\equiv CPh)Cl(Py)_2(CO)$	2.244(6)	1.408(8)	21
$Cr(MA)(CO)_2(\eta^6\text{-}C_6H_3Me_3)$	2.177(8)	1.43(1)	22
$Mo(MA)(CO)_2(\eta^6\text{-}C_6Et_6)$	2.28(2)	1.49(2)	23
$W(MA)(PhC\equiv CH)(S_2CNMe_2)$	2.247(8)	1.41(1)	24

[a] This work. [b] R = *p*-tolyl.

zene resulted in a rapid change of the colour of the solution from green to orange. The complex formed analysed correctly for $Os(C_2F_4)Cl(NO)(PPh_3)_2$ (Eq. 6).

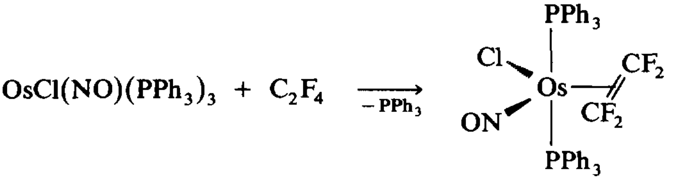

(6)

^{31}P NMR confirmed the existence of only one isomer in solution. The ^{13}C NMR identified that isomer as being the one with *trans* triphenylphosphine ligands since the *ipso* carbon for the PPh_3 ligand was a triplet, due to virtual coupling between the phosphorus atoms. Also, there were two carbon signals present for the carbons of the C_2F_4 group. The chemical shifts of the two inequivalent CF_2 carbons (due to different *trans* groups i.e. Cl or NO) occurred at 118.7 ppm and 102.5 ppm. Both of these carbon signals were split, by the two fluorines bound to them, into triplets ($^1J(CF) = 321.2$ Hz and $^1J(CF) = 315.1$ Hz) (Table 5). Again there was no resolvable coupling to the fluorines of the adjacent carbon. The ^{19}F NMR spectrum also clearly showed the inequivalence of the two CF_2 groups, with two sets of multiplets (-113.1 and -103.3 ppm). The ^{31}P NMR spectrum of $Os(C_2F_4)Cl(NO)(PPh_3)_2$ was found to be temperature invariant from -50 to $80\,°C$ and was stable with respect to loss of C_2F_4. There was, therefore, no evidence for any other isomers of $Os(C_2F_4)Cl(NO)(PPh_3)_2$. A preliminary X-ray investigation has confirmed the *trans* phosphine arrangement for $Os(C_2F_4)Cl(NO)(PPh_3)_2$ in the solid state but the data collected was not of sufficient quality to enable complete structure solution.

$OsCl(NO)(PPh_3)_3$ reacted rapidly with maleic anhydride under the same conditions with which the tetrafluoroethylene adduct was formed (Eq. 7).

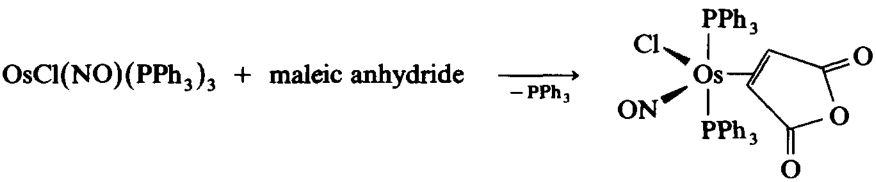

(7)

As with $Os(C_2F_4)Cl(NO)(PPh_3)_2$, the maleic anhydride adduct complex also exists as the isomer with *trans* PPh_3 ligands. The ^1H NMR spectrum, however, showed only a single broad resonance for the olefinic protons (Table 6). These protons would be expected to appear as two signals at different chemical shifts if the maleic anhydride ligand was static. Therefore the maleic anhydride must be undergoing motion on the NMR timescale which results in an averaging of the signals. This behaviour is also seen for the ethylene complexes $Os(C_2H_4)(CO)_2(PPh_3)_2$ [4] and $Os(C_2H_4)Cl(NO)(PPh_3)_2$ [28]. The ^{13}C NMR spectrum also confirmed this dynamic behaviour, as the *ipso* carbons of the PPh_3 groups were triplets due to virtual coupling of the phosphorus atoms. If the maleic ahydride ligand was in a fixed conformation the phosphorus atoms would be inequivalent. The equivalence of the PPh_3 groups was also evident in the ^{13}P spectrum, with only a singlet being observed. Why the maleic anhydride ligand shows this dynamic behaviour is not understood.

Tetrafluoroethylene complexes of $M(CO)(CNR)(PPh_3)_2$ ($M = Os, Ru$)

Both $Ru(CO)(CNR)(PPh_3)_3$ and $Os(CO)(CNR)(PPh_3)_3$ reacted with tetrafluoroethylene to give good yields of pure mono adducts of the form $M(C_2F_4)(CO)(CNR)(PPh_3)_2$ (M = Ru, Os) (Eq. 8). $Ru(CO)(CNR)(PPh_3)_3$ was photolysed under an atmosphere of C_2F_4 until the red colour had completely faded (3–4 hours). These were much more vigorous conditions than were required for the related dicarbonyl species, $Ru(CO)_2(PPh_3)_3$. All of the osmium complexes, except $OsCl(NO)(PPh_3)_3$, required vigorous conditions to displace the third triphenylphosphine. $Os(CO)(CNR)(PPh_3)_3$ was heated at 90 °C for 48 hours under pressure of 500 kPa of C_2F_4, to complete reaction.

$M(CO)(CNR)(PPh_3)_3 \xrightarrow[-PPh_3]{C_2F_4}$ 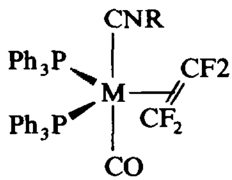 (8)

(M = Ru, Os R = *p*-Tolyl)

In solution these complexes exist as one isomer only. This isomer has the geometry with *cis* triphenylphosphines along with the tetrafluoroethylene ligand in the equatorial plane. The carbonyl and isocyanide groups occupy the axial sites. This geometry was confirmed by ^{13}C NMR. As with most of the *cis* phosphine complexes, the *ipso* carbon of the PPh_3 ligand was a doublet (Ru, $^1J(CP) = 34.4$ Hz; Os $^1J(CP) = 44.4$ Hz). The carbons of the tetrafluoroethylene both exhibited the coupling pattern expected for a ^{13}C coupled to two inequivalent fluorines and a single *trans* phosphorus atom (ddd). Other couplings could not be resolved.

Maleic anhydride adduct of $Ru(CO)(CNR)(PPh_3)_3$

The zero-valent complex $Ru(CO)(CNR)(PPh_3)_3$ undergoes ligand substitution reactions with a number of unsaturated species [27]. The geometry of the resulting π-adducts is apparently dependent upon the nature of the coordinating ligand. Thus carbon disulfide and oxygen give complexes which result in a *trans* configuration of the triphenylphosphine ligands [27] (Fig. 5). Adducts with maleic anhydride (MA), fumaronitrile (FN), maleonitrile (MN), and dimethylfumarate (DF), have *cis* triphenylphosphine ligands [7,8] (Fig. 5). The structure of $Ru(MA)(CO)(CNR)(PPh_3)_2$ has been determined [8]. The ruthenium is five coordinate, with the maleic anhydride and the triphenylphosphines occupying the equatorial plane. The CNR and CO ligands are coordinated in the axial positions. Unexpectedly, the maleic anhydride ligand adopts the position adjacent to the more bulky *p*-tolylisocyanide ligand.

Solution structure of $Ru(MA)(CO)(CNR)(PPh_3)_2$

The ^1H NMR of $Ru(MA)(CO)(CNR)(PPh_3)_2$ had been reported previously and the complex was described as rigid in solution [7]. A re-investigation of the ^1H NMR showed the reported doublet at 3.18 ppm. On closer examination, other multiplets were also identifiable (3.12(dd), 3.08(dd), 2.87(d) and 2.93(d)). These signals were attributed to at least 3 other geometric isomers of $Ru(MA)(CO)(CNR)(PPh_3)_2$. However, the ^1H NMR spectrum was not helpful in assigning the structures of these isomers. Their structures were determined using ^{31}P and ^{13}C NMR spectroscopy and were found to be those isomers formed by simple Berry rotation of the trigonal bipyramidal $Ru(MA)(CO)(CNR)(PPh_3)_2$ (Scheme 1). The relative

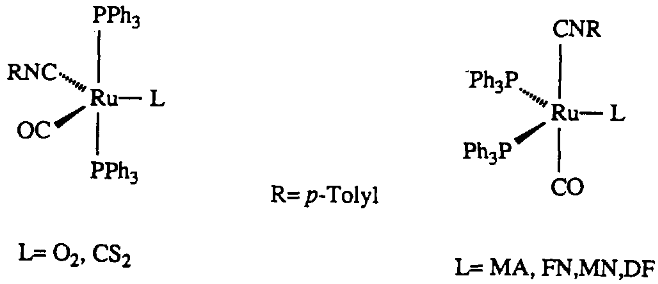

Fig. 5.

geometry of the maleic anhydride was intentionally omitted in the structures in Scheme 1 as this was not determined.

The ^{13}C NMR spectrum showed the presence of these other isomers and allowed the assignment of the stereochemistry of the major ones. It was possible to completely assign the structures of two of the four isomers which could be seen in solution. The aromatic region was highly complex but several features could be seen. A number of signals attributed to *ipso* carbons for the triphenylphosphine ligands were observed. The major isomer showed a non-first order pattern at 136.8 ppm. There was also a triplet and several doublets which could not be assigned to any particular isomer. The *ipso* carbon at 136.8 ppm was assigned to the complex (A), with the geometry observed in the crystal structure.

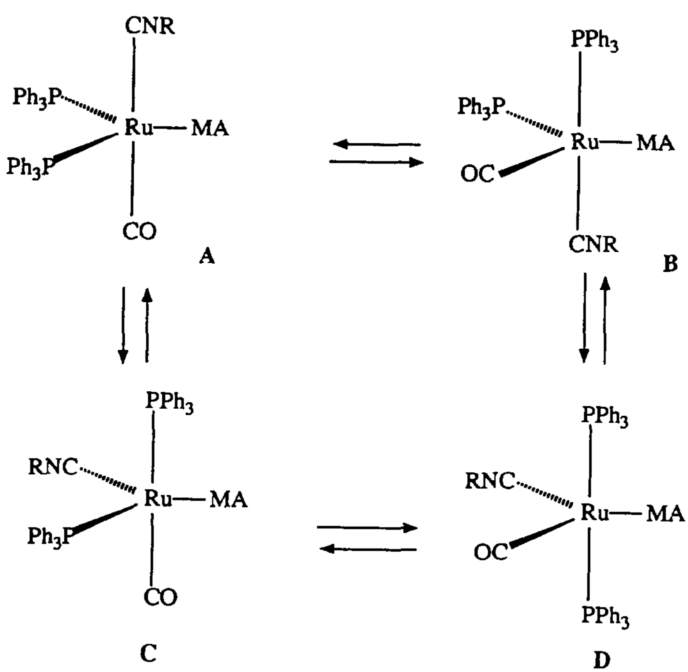

Scheme 1

Three types of olefinic carbons could be identified (37.8(dd), 34.95(dd) and 33.7(m) ppm). The signal assigned to the most abundant isomer (**A**) (33.7 ppm) was non-first order. The other two had a coupling pattern similar to that of the olefinic carbons in $Ru(MA)(CO)_2(PPH_3)_2$ and were therefore assigned to an isomer with *cis* inequivalent triphenylphosphine groups (**B**). Analysis of the anhydride carbonyl carbon resonances gave the same result (i.e. two major isomers in solution assigned as **A** and **B**.

The carbonyl ligand carbon resonance is a clean triplet for isomer **A** (164 ppm $^2J(PC) = 17$ Hz) as expected for coupling to two equivalent *cis* phosphorus atoms. Isomer **B** (162.7 ppm), however, appeared as a complex multiplet which probably arose from the coupling of the carbonyl carbon to two inequivalent *cis* phosphorus atoms. What allowed unequivocal assignment of the second major isomer as the structure **B**, was the signal due to the CNR carbon. This carbon gave rise to a triplet for isomer **A** (203.2 ppm, $^2J(CP) = 13$ Hz) but a doublet for the other major isomer **B** (206.4 ppm $^2J(CP) = 21$ Hz). A $^2J(CP)$ value of this magnitude indicated that the isocyanide carbon was *trans* to a triphenylphosphine group.

The ^{31}P NMR spectrum was the most telling evidence for the presence of four isomers (**A,B,C,D**) in solution. The two major species appeared to be present in approximately a 1:1 ratio (as seen in the ^{13}C and ^1H NMR). Isomer **A** gave a singlet at 40.18 ppm, with isomer **B** showing two doublets at 39.24 and 34.26 ppm with a $^2J(PP)$, of 24.0 Hz. Also identifiable was another isomer with two separate phosphine signals (33.85 and 29.97 ppm) with a $^2J(PP')$ of 24.6 Hz. This spectrum was assigned as being that of isomer **C**. Lastly, another coupled pair of resonances were found at 38.5 and 26.3 ppm with a $^2J(PP')$ of 359 Hz. This large value for $^2J(PP')$ must be due to coupling of *trans* inequivalence phosphorus atoms, the inequivalence being induced in the PPh_3 ligands by the maleic anhydride being closer to one triphenylphosphine than the other.

This equilibrium was much more complicated than the simple *cis–trans* isomerisation observed for $Os(C_2F_4)(CO)_2(PPh_3)_2$. These isomerisations were again slow on the ^{31}P NMR time-scale with all of the isomers observed giving sharp spectra. The existence of so many geometric isomers of $Ru(MA)(CO)(CNR)(PPh_3)_2$ in solution indicated that the energy differences between the different isomers was very small.

Conclusions

The tendency for many five coordinate ruthenium or osmium d^8 complexes (of the type $M(L)(CO)(L')(PPh_3)_2$ L = unsaturated molecule; L′ = CO, CNR, CS; M = Ru, Os) to adopt geometries in which the triphenylphosphine ligands are *trans*, has been considered to be a consequence mainly of steric effects. The extension of L to more electron withdrawing olefins has shown that the "steric" replusion of the triphenylphosphine ligands is not as important as previously thought. For less π-accepting ligands, such as O_2, C_2H_4 and CS_2, the steric constraints of the PPh_3 groups dominated and, therefore, these complexes all had a geometry with *trans* triphenylphosphine ligands.

The more π-accepting olefins such as tetrafluoroethylene and maleic anhydride provide sufficient electronic influence to counter the steric effects of the PPh_3 groups. The effect of changing the π-accepting characteristics of the olefin can be

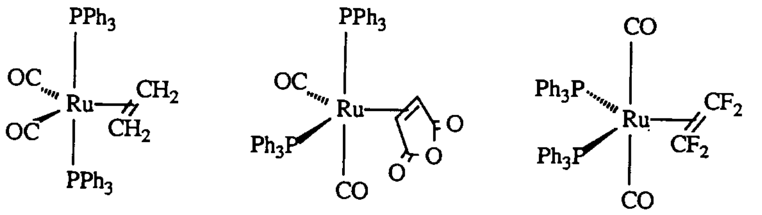

Fig. 6.

seen when the series $Ru(L)(CO)_2(PPh_3)_2$ ($L = C_2H_4$, MA, C_2F_4) is considered (Fig. 6). The complex $Ru(C_2H_4)(CO)_2(PPh_3)_2$ [26] has a very poorly π-accepting olefin coordinated and the steric pressure of the PPh_3 groups dominate its geometry. Upon moving to a more π-accepting olefin the geometry changes. The complex $Ru(MA)(CO)_2(PPh_3)_2$, if it were to exist as the same structure as $Ru(C_2H_4)(CO)_2(PPh_3)_2$, would have three good π-accepting ligands competing for the electron density in the equatorial plane. This electronic competition would be relieved if a phosphine ligand was brought into the equatorial plane and a carbonyl was moved to an axial site. This would do two things: an electron-donating ligand would be brought into the same plane as the maleic anhydride ligand, and another π-acceptor is removed from competing directly for the same electron density as the olefin. This would result in more electron density being available to the π^* orbital of the olefin.

In the case of tetrafluoroethylene, the removal of one carbonyl group from the equatorial plane is not sufficient to provide enough electron density for the olefin. In $Ru(C_2F_4)(CO)_2(PPh_3)_2$ the tetrafluoroethylene is such a strong π-acceptor that it requires both the σ-donating phosphine ligands in the same plane, as well as the carbonyl ligands removed from that plane.

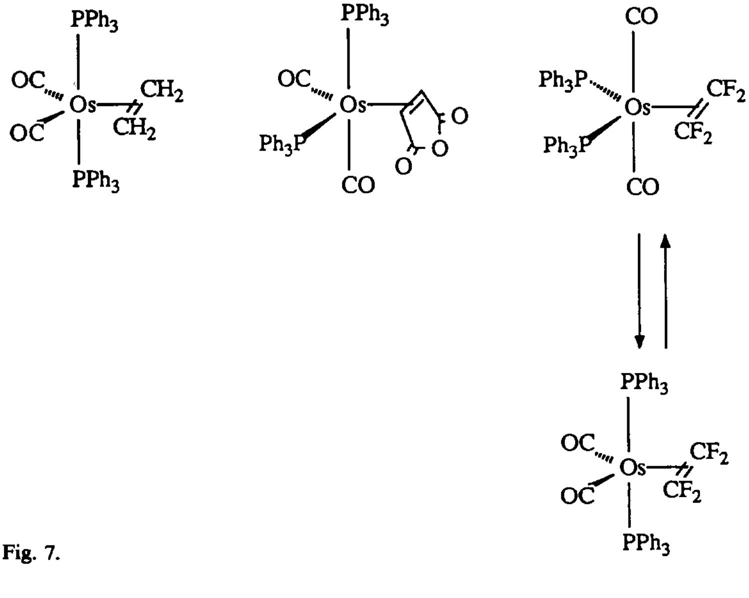

Fig. 7.

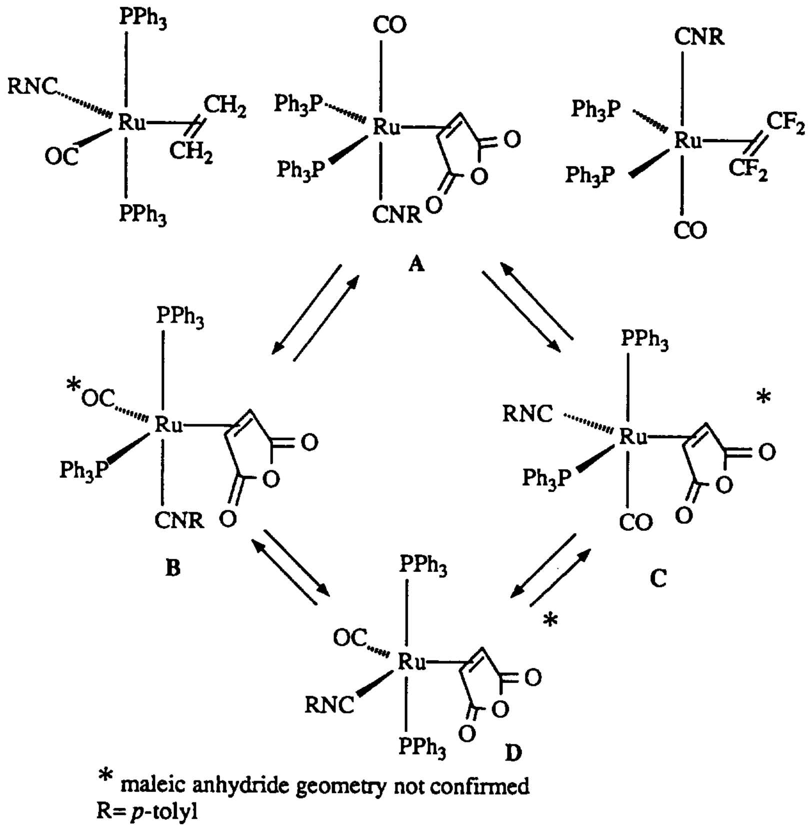

Fig. 8.

The same type of pattern exists for the osmium series $Os(L)(CO)_2(PPh_3)_2$ ($L = C_2H_4$, MA, C_2F_4) (Fig. 7). The situation here, is not as clear as for the ruthenium example above. Both the ethylene and maleic anhydride complexes behave in the same way as their ruthenium analogues. The tetrafluoroethylene complex on the other hand interconverts (in solution) between the isomer with *cis* carbonyl and *trans* carbonyl ligands, with no evidence for the geometry which was observed when L = maleic anhydride. Also, $\Delta H°$ shows there is very little energy difference between the two isomers.

It should be noted that neither $Os(MA)(CO)_2(PPh_3)_2$ nor $Os(C_2F_4)(CO)_2(PPh_3)_2$ shows any evidence of free rotation of the olefin. In contrast, the ethylene ligand in $Os(C_2H_4)(CO)_2(PPh_3)_2$ undergoes rapid free-rotation about the metal—olefin bond. The ^1H spectrum for $Os(C_2H_4)(CO)_2(PPh_3)_2$ has a clear 1:3:1 triplet for the olefinic protons [4]. As all of the protons on the olefin are magnetically inequivalent, the spectrum would be significantly more complex if the olefin was in a locked conformation. Rapid free-rotation of the ethylene would result in all of the protons becoming equivalent, giving rise to the observed spectrum. The barrier to free-rotation of the ethylene in $Os(C_2H_4)(CO)_2(PPh_3)_2$ must be low as the spectrum showed no significant change in dropping the temperature to $-50°C$.

The last series of complexes is that of the more electron-rich metal centre $Ru(L)(CO)(CNR)(PPh_3)_2$ ($L = C_2H_4$, MA, C_2F_4) (Fig. 8). The two extremes of electronic character in the olefins, i.e., ethylene and tetrafluoroethylene, give complexes of the same general geometry as were found for the related complexes $Ru(C_2H_4)(CO)_2(PPh_3)_2$ [27] and $Ru(C_2F_4)(CO)_2(PPh_3)_2$. The intermediate case of $Ru(MA)(CO)(CNR)(PPh_3)_2$ exists as at least four isomers in solution. The increased electron density at the ruthenium centre must result in the available geometries for the maleic anhydride complex having almost no energy difference. This, and the usual lability of five-coordinate complexes may explain why all isomers are observable.

Experimental

General

Standard Schlenk techniques were used for all manipulations involving oxygen- or moisture-sensitive compounds. Solvents used were purified as follows: benzene, toluene, THF, diethyl ether and n-hexane were distilled from sodium/benzophenone; dichloromethane and acetonitrile were distilled from calcium hydride.

When procedures involved materials that were not air-sensitive, solvents were purified by chromatography on alumina (Spence type H, 100-200 mesh) or filtered prior to use. In these cases, solvent removal under reduced pressure was achieved using a rotary evaporator. Routine recrystallizations were achieved by the following method: The sample was dissolved in a low boiling-point solvent and a higher boiling-point solvent, in which the compound was insoluble, was added. Evaporation at reduced pressure effected gradual crystallization.

Infrared spectra (4000–200 cm^{-1}) were recorded on a Perkin–Elmer Model 597 double-beam spectrophotometer calibrated with polystyrene film. All spectra were recorded as Nujol mulls between KBr plates or as dichloromethane solutions in KBr cells. Far-infrared spectra (400–200 cm^{-1}) were recorded as concentrated Nujol mulls between CsI plates. ^1H NMR were recorded on a Bruker AM-400 spectrometer operating at 400 MHz and are quoted in ppm down-field from TMS. $^{13}C\{^1H\}$ NMR were recorded on a Bruker AM-400 at 100 MHz and are quoted relative to TMS. $^{31}P\{^1H\}$ NMR were recorded on a Bruker AM-400 at 162 MHz and are quoted relative to 85% phosphoric acid solution (external). ^2H NMR were recorded on a Bruker AM-400 at 61.4 MHz and referenced using $CDCl_3$ (7.26 ppm). ^{19}F NMR were recorded on a Jeol FX-90 at 84.6 MHz and reported relative to $CFCl_3$. Melting points were determined on a Reichert microscope hot-stage and are uncorrected. Elemental analyses for carbon, hydrogen, nitrogen and fluorine were performed by the Microanalytical Laboratory of the University of Otago. $Ru(CO)_2(PPh_3)_3$ [26], $Os(CO)_2(PPh_3)_3$ [27], Ru(CN-*p*-tolyl)(CO)$(PPh_3)_3$ [27], Os(CN-*p*-tolyl)(CO)$(PPh_3)_3$ [27] and $OsCl(NO)(PPh_3)_3$ [28] were all prepared by standard literature procedures. Tetrafluoroethylene was prepared by vacuum pyrolysis of poly(tetrafluoroethylene) [29]. Spectral data are given for all new compounds in Tables 1, 5, 6 and 7.

Reactions

$Ru(C_2F_4)(CO)_2(PPh_3)_2$

(a) $Ru(CO)_2(PPh_3)_2$ (1 g, 1.55 mmol) was dissolved in degassed benzene (40 mL) and stirred under tetrafluoroethylene pressure (300 kPa) in a Fischer–Porter bottle (volume 300 mL), until the yellow colour was discharged. The C_2F_4 was then vented and the solution filtered. Ethanol (50 mL) was added to the filtrate and the benzene removed under reduced pressure to give the product as white crystals (754 mg, 62%). m.p. 168–172 °C. Anal. Found: C, 60.53; H, 4.37; F, 8.75. $C_{40}H_{30}F_4O_2P_2Ru$ calcd.: C, 61.46; H, 3.86; F, 9.72%.

(b) $Ru(CO)_3(PPh_3)_2$ (200 mg, 0.3 mmol) was dissolved in degassed benzene (10 mL) and heated at 90 °C for 24 hours under tetrafluoroethylene pressure (500 kPa) in a Carius tube. The C_2F_4 was then vented and the solution filtered. Ethanol (30 mL) was added to the filtrate and the benzene removed at reduced pressure to give the product as white crystals (192 mg, 87%).

(c) $Ru(C_2H_4)(CO)_2(PPh_3)_2$ (200 mg, 0.3 mmol) was dissolved in degassed benzene (10 mL) and stirred for 24 h under tetrafluoroethylene pressure (500 kPa) in a Fischer-Porter bottle (volume 300 mL). The C_2F_4 was then vented and the solution filtered. Ethanol (30 mL) was added to the filtrate and the benzene removed under reduced pressure to give the product as white crystals (161 mg, 73%).

$Ru(C_2F_4)(CO)(CN$-p-$tolyl)(PPh_3)_2$

$Ru(CO)(CN$-*p*-$tolyl)(PPh_3)_3$ (700 mg, 0.68 mmol) was dissolved in degassed benzene (40 mL) and stirred under tetrafluoroethylene pressure (300 kPa) in a Fischer-Porter bottle (volume 300 mL). The solution was irradiated with a 1000 watt halogen lamp until the red colour was discharged. The C_2F_4 was then vented and the solution filtered. Ethanol (50 mL) was added to the filtrate and the benzene removed under reduced pressure to give the product as cream crystals (537 mg, 90%). m.p. 126–129 °C. Anal. Found: C, 64.99; H, 5.07; N, 1.34; F, 7.81 $C_{47}H_{37}F_4NOP_2Ru$ calcd.: C, 64.83; H, 4.28; N, 1.61; F, 8.73%.

$Os(C_2F_4)Cl(NO)(PPh_3)_2$

$OsCl(NO)(PPh_3)_3$ (1 g, 0.96 mmol) was dissolved in degassed benzene (10 mL) and stirred under tetrafluoroethylene pressure (500 kPa) in a Fischer-Porter bottle (volume 300 mL) until the green colour had completely gone. The C_2F_4 was then vented and the solution filtered. Ethanol (30 mL) was added to the filtrate and the benzene removed under reduced pressure to give the product as orange crystals (810 mg, 96%). m.p. 185–187 °C. Anal. Found: C, 52.03; H, 3.84; F, 8.26 $C_{38}H_{30}ClF_4NOOsP_2$ calcd.: C, 52.81; H, 3.50; F, 8.79%.

$Os(C_2F_4)(CO)_2(PPh_3)_2$

$Os(CO)_2(PPh_3)_3$ (1 g, 0.97 mmol) was dissolved in degassed benzene (10 mL) and heated at 90 °C for 24 h under tetrafluoroethylene pressure (at approximately 500 kPa) in a Carius tube. The C_2F_4 was then vented and the solution filtered. Ethanol (30 mL) was added to the filtrate and the benzene removed under reduced pressure to give the product as white crystals (700 mg, 83%). m.p. 203–207 °C. Anal. Found: C, 53.61; H, 3.82; F, 7.76. $C_{40}H_{30}F_4O_2OsP_2$ calcd.: C, 53.26; H, 3.42; F, 8.32%.

$Os(C_2F_4)(CO)(CN$-p-$tolyl)(PPh_3)_2$

$Os(CO)(CNR)(PPh_3)_3$ (800 mg, 0.71 mmol) was dissolved in degassed benzene

(40 mL) and heated under tetrafluoroethylene pressure (at approximately 500 kPa) in a Carius tube at 90 °C for 24 h. The C_2F_4 was then vented and the solution filtered. Ethanol (50 mL) was added to the filtrate and the benzene removed under reduced pressure to give the product as pale yellow crystals (582 mg, 85%). m.p. 227–230 °C. Anal. Found: C, 58.67; H, 4.08; N, 1.37; F, 8.00. $C_{47}H_{37}F_4NOOsP_2$ calcd.: C, 58.80; H, 3.89; N, 1.46; F, 7.92%.

$Os(C_2F_4)(CO)(CS)(PPh_3)_2$

$Os(CO)(CS)(PPh_3)_3$ (500 mg, 0.48 mmol) was dissolved in degassed benzene (40 mL) and heated under tetrafluoroethylene pressure (at approximately 500 kPa) in a Carius tube at 90 °C for 24 h. The C_2F_4 was then vented and the solution filtered. The benzene was removed in vacuo and the residue subjected to column chromatography on silica, elution being with dichloromethane. The first band from the column was collected and recrystallized with ethanol to give the product as yellow crystals (181 mg, 43%). m.p. 168–170 °C. Anal. Found: C, 54.30; H, 4.05. $C_{40}H_{30}F_4OOsP_2S$ calcd.: C, 54.17; H, 3.41%.

Ru(maleic anhydride)$(CO)_2(PPh_3)_2$

$Ru(CO)_2(PPh_3)_3$ (500 mg, 0.5 mmol) was dissolved in degassed benzene (10 mL) containing maleic anhydride (48 mg, 0.5 mmol). The solution was stirred until the colour faded. The benzene was removed in vacuo and the residue recrystallised from dichloromethane and ethanol to give the product as colourless crystals (317 mg, 81%). mp. 165–168 °C. Anal. Found: C, 64.63; H, 4.57 $C_{42}H_{32}O_5P_2Ru$ calcd.: C, 64.70; H, 4.14%.

Os(maleic anhydride)$(CO)_2(PPh_3)_2$

$Os(C_2H_4)(CO)_2(PPh_3)_3$ (500 mg, 0.6 mmol) was dissolved in degassed benzene (10 mL) containing maleic anhydride (60 mg, 0.6 mmol). The solution was stirred at reflux temperature for 2 h. The benzene was then removed in vacuo and the residue recrystallised from dichloromethane and ethanol to give the product as colourless crystals (382 mg, 70%). m.p. 153–156 °C. Anal. Found: C, 58.03; H, 4.04. $C_{42}H_{32}O_5OsP_2$ calcd.: C, 58.06; H, 3.71%.

Os(maleic anhydride)Cl(NO)$(PPh_3)_2$

$OsCl(NO)(PPh_3)_3$ (500 mg, 0.5 mmol) was dissolved in degassed benzene (40 mL) containing maleic anhydride (48 mg, 0.5 mmol). The solution was stirred until the green colour had completely faded. The benzene was removed in vacuo and the residue recrystallised from dichloromethane and ethanol to give the product as orange crystals (400 mg, 91%). m.p. 165–168 °C. Anal. Found: C, 54.93; H, 4.42; N, 1.36. $C_{40}H_{32}ClNO_4OsP_2$ calcd.: C, 54.70; H, 3.67; N, 1.59%.

X-Ray collection and refinement

Crystals suitable for data collection were mounted on glass fibres and positioned on a Nonius CAD-4 diffractometer. Unit cell dimensions were derived from least-squares fits to the observed setting angles of 25 refections, using monochromated Mo-K_α ($\lambda = 0.7107$ Å) for $Ru(C_2F_4)(CO)_2(PPh_3)_2$ and Cu-K_α ($\lambda = 1.5418$ Å) for $Os(MA)(CO)_2(PPh_3)_2$. Crystal alignment and decomposition were monitored throughout data collection by measuring three standard reflections every 100

Table 11

Crystal data and details of the structure determinations of $Ru(C_2F_4)(CO)_2(PPh_3)_2$ and $Os(MA)(CO)_2(PPh_3)_2$

	$Ru(C_2F_4)(CO)_2(PPh_3)_2$	$Os(MA)(CO)_2(PPh_3)_2$
Crystal data		
formula	$C_{40}H_{30}F_4P_2O_2Ru$	$C_{42}H_{32}P_2O_5Os$
molecular weight (g mol^{-1})	781.7	868.9
space group	$P2_1/a$	$P2_1/c$
crystal system	monoclinic	monoclinic
a (Å)	35.940(2)	23.667(2)
b (Å)	10.655(7)	20.306(1)
c (Å)	18.559(6)	16.147(1)
β (°)	93.21(3)	93.20(1)
V (Å^3)	7095	7748
Z	8	8
d (calcd) (g cm^{-3})	1.464	1.490
$F(000)$	2928	3440
μ (cm^{-1})	5.8	74.0
Data collection and reduction		
diffractometer	Nonius CAD-4	Nonius CAD-4
radiation	Mo-K_α (λ = 0.7107 Å)	Cu-K_α (λ = 1.5418 Å)
temperature (K)	294–296	294–296
scan technique	$2\theta/\omega$	$2\theta/\omega$
2θ(min-max) (°)	2–46	2–63
scan speed (° min^{-1})	2–30	2–30
no. unique refections	6870	9906
no. unique obsd. reflections	2981	5172
σ criterion	3.0	3.0
R_{MERG}	0.070	0.035
Structure determination and refinement		
R and R_w [a]	0.096, 0.099	0.070, 0.074
weight	$0.2237/(\sigma^2(F)+0.071088F^2)$	$1.80856/(\sigma^2(F)+0.003662F^2)$

[a] $R=\Sigma|(|F_o|-|F_c|)|/\Sigma|F_o|$. $R_w=[\Sigma_w(|F_o|-|F_c|)^2/\Sigma_w|F_o|^2]^{1/2}$.

measurements, no non-statistical variation being observed. The data were corrected for Lorentz and polarisation effects and equivalent reflections averaged. Absorption corrections were applied by the empirical azimuthal method [30], with the maximum and minimum corrections for $Ru(C_2F_4)(CO)_2(PPh_3)_2$ being 1/0.82 and 1/0.99 and for $Os(MA)(CO)_2(PPh_3)_2$ being 1/0.74 and 1/0.99 respectively. Computing was carried out by using the SDP suite of programmes on a PDP-11 for inital data processing, and SHELX-76, on an IBM 4341, for structure solution and refinement. Details of crystal data and intensity data collection parameters are summarised along with atom positions in Tables 11, 12, and 13. Atomic scattering factors were for neutral atoms. F_{obs} and F_{calc} together with the anisotropic thermal parameters are available from the authors.

Table 12

Atomic coordinates for $Ru(C_2F_4)(CO)_2(PPh_3)_2$

	Molecule 1			Molecule 2		
	x	*y*	*z*	*x*	*y*	*z*
Ru	0.1226(1)	0.5627(2)	0.0485(1)	0.1256(1)	0.8062(2)	0.5500(4)
P1	0.1367(2)	0.3930(7)	−0.0336(4)	0.1394(2)	0.9767(7)	0.4677(3)
P2	0.1106(2)	0.4482(8)	0.1568(4)	0.1146(2)	0.9210(7)	0.6591(3)
C1	0.1263(9)	0.7331(30)	−0.0032(17)	0.1297(9)	0.6321(32)	0.5002(18)
C2	0.1164(8)	0.7596(27)	0.0706(14)	0.1212(9)	0.6181(33)	0.5746(18)
F1	0.1592(7)	0.7912(15)	−0.0139(8)	0.1633(6)	0.5773(17)	0.4823(10)
F2	0.1034(8)	0.7803(21)	−0.0525(10)	0.1037(6)	0.5848(17)	0.4503(9)
F3	0.0825(7)	0.8054(18)	0.0822(11)	0.0845(7)	0.5688(17)	0.5853(11)
F4	0.1412(7)	0.8110(14)	0.1162(10)	0.1458(7)	0.5537(16)	0.6204(9)
C3	0.0690(10)	0.5684(31)	0.0287(18)	0.0723(7)	0.8022(24)	0.5326(13)
O3	0.0379(7)	0.5768(31)	0.0203(15)	0.0420(6)	0.7924(26)	0.5195(12)
C4	0.1737(9)	0.5795(27)	0.07324(15)	0.1785(9)	0.7914(27)	0.5765(15)
O4	0.2052(7)	0.5948(25)	0.0876(12)	0.2080(6)	0.7742(23)	0.5909(15)
C11	0.0973(7)	0.2968(23)	−0.0756(13)	0.1021(7)	1.0670(23)	0.4279(13)
C12	0.0672(8)	0.3691(28)	−0.0969(15)	0.0698(8)	1.0042(28)	0.4019(15)
C13	0.0352(10)	0.3135(36)	−0.1327(21)	0.0369(9)	1.0703(31)	0.3714(17)
C14	0.0380(9)	0.1664(30)	−0.1377(17)	0.0379(9)	1.1932(35)	0.3692(19)
C15	0.0682(10)	0.1056(34)	−0.1164(19)	0.0719(10)	1.2693(33)	0.3914(18)
C16	0.0987(8)	0.1676(27)	−0.0886(15)	0.1023(8)	1.2047(29)	0.4209(16)
C21	0.1603(6)	0.4293(22)	−0.1128(12)	0.1633(7)	0.9196(22)	0.3838(12)
C22	0.1682(8)	0.5586(26)	−0.1280(15)	0.1674(9)	0.8003(32)	0.3692(18)
C23	0.1873(8)	0.5965(27)	−0.1912(15)	0.1848(9)	0.7650(31)	0.3037(17)
C24	0.1985(9)	0.5055(31)	−0.2370(17)	0.1976(8)	0.8670(28)	0.2606(15)
C25	0.1921(8)	0.3775(27)	−0.2219(15)	0.1924(10)	0.9816(34)	0.2746(18)
C26	0.1698(7)	0.3489(25)	−0.1618(15)	0.1759(7)	1.0263(26)	0.3391(15)
C31	0.1691(8)	0.2756(26)	0.0048(15)	0.1730(7)	1.0881(24)	0.5070(14)
C32	0.2072(8)	0.3020(28)	−0.0013(16)	0.2124(9)	1.061(30)	0.5029(17)
C33	0.2351(10)	0.2195(35)	0.0374(20)	0.2374(8)	1.1462(29)	0.5375(16)
C34	0.2187(10)	0.1058(31)	0.0770(18)	0.2254(8)	1.2502(29)	0.5744(16)
C35	0.1838(8)	0.0908(28)	0.0747(16)	0.1880(8)	1.2746(27)	0.5764(15)
C36	0.1570(8)	0.1716(27)	0.0450(15)	0.1609(7)	1.1949(25)	0.5456(14)
C41	0.0791(7)	0.5370(25)	0.2130(14)	0.0825(6)	0.8368(22)	0.7145(12)
C42	0.0461(7)	0.4774(23)	0.2397(13)	0.0517(7)	0.8853(24)	0.7390(13)
C43	0.0238(8)	0.5568(29)	0.2829(16)	0.0300(9)	0.8112(30)	0.7869(17)
C44	0.0344(8)	0.6727(28)	0.2989(16)	0.0389(7)	0.6865(25)	0.8048(13)
C45	0.0634(7)	0.7226(26)	0.2713(14)	0.0729(8)	0.6325(28)	0.7814(15)
C46	0.0879(9)	0.6623(32)	0.2281(18)	0.0915(7)	0.7131(24)	0.7320(14)
C51	0.0886(7)	0.2925(24)	0.1505(14)	0.0922(6)	1.0802(20)	0.6496(11)
C52	0.1010(9)	0.1864(31)	0.1997(17)	0.1029(8)	1.1692(28)	0.6920(16)
C53	0.0800(10)	0.0732(33)	0.1752(19)	0.0892(9)	1.2982(30)	0.6925(17)
C54	0.0558(9)	0.0654(31)	0.1222(18)	0.0610(10)	1.3208(35)	0.6397(20)
C55	0.0453(10)	0.1513(34)	0.0836(19)	0.0493(8)	1.2160(29)	0.5898(16)
C56	0.0616(9)	0.2810(32)	0.0873(18)	0.0657(8)	1.0946(28)	0.5973(16)
C61	0.1503(6)	0.4184(21)	0.2211(12)	0.1545(6)	0.9486(22)	0.7231(12)
C62	0.1497(7)	0.4456(25)	0.2939(15)	0.1514(7)	0.9340(24)	0.7993(14)
C63	0.1767(8)	0.4019(29)	0.3437(16)	0.1819(9)	0.9650(29)	0.8455(16)
C64	0.2106(8)	0.3497(30)	0.3174(17)	0.2100(9)	1.0194(32)	0.8200(17)
C65	0.2122(10)	0.3219(33)	0.2433(19)	0.2141(8)	1.0373(27)	0.7440(15)
C66	0.1817(9)	0.3616(30)	0.1933(17)	0.1855(7)	1.0048(23)	0.6980(13)

Table 13

Atomic coordinates for $Os(MA)(CO)_3(PPh_3)_2$

	Molecule 1			Molecule 2		
	x	*y*	*z*	*x*	*y*	*z*
Os	0.06805(4)	0.15605(4)	0.24777(5)	0.58650(4)	0.08057(6)	0.22927(6)
P1	0.1260(2)	0.0588(3)	0.2568(3)	0.6197(2)	−0.0087(3)	0.1421(4)
P2	0.1115(2)	0.2080(3)	0.1287(3)	0.6383(2)	0.0570(3)	0.3589(4)
O1	0.0033(9)	0.1271(1)	0.402(1)	0.550(1)	0.215(1)	0.280(1)
O2	0.1344(6)	0.2586(9)	0.349(1)	0.6630(9)	0.168(1)	0.132(1)
O3	−0.0514(6)	0.0214(7)	0.197(1)	0.4421(7)	0.149(1)	0.137(1)
O4	−0.0868(6)	0.2272(8)	0.266(1)	0.4482(7)	0.110(1)	0.270(1)
O5	−0.0756(5)	0.1198(7)	0.246(1)	0.4634(8)	0.048(1)	0.381(1)
C1	0.027(1)	0.133(1)	0.344(2)	0.565(1)	0.164(1)	0.264(2)
C2	0.109(1)	0.220(1)	0.314(2)	0.636(1)	0.135(1)	0.167(2)
C3	−0.0108(8)	0.187(1)	0.181(1)	0.503(1)	0.059(2)	0.172(2)
C4	0.0010(7)	0.1195(9)	0.161(1)	0.5122(8)	0.022(1)	0.253(1)
C5	−0.041(1)	0.078(1)	0.198(2)	0.475(1)	0.055(1)	0.309(2)
C6	−0.060(1)	0.184(1)	0.233(1)	0.459(1)	0.107(2)	0.187(2)
C11	0.1995(8)	0.061(1)	0.305(1)	0.581(1)	−0.088(1)	0.134(1)
C12	0.2133(9)	0.113(1)	0.359(1)	0.566(1)	−0.115(1)	0.059(1)
C13	0.267(1)	0.117(1)	0.400(2)	0.545(1)	−0.178(2)	0.051(2)
C14	0.306(1)	0.068(1)	0.384(2)	0.540(1)	−0.214(2)	0.126(2)
C15	0.291(1)	0.015(1)	0.334(2)	0.559(1)	−0.189(2)	0.207(2)
C16	0.237(1)	0.011(1)	0.295(1)	0.577(1)	−0.122(1)	0.209(2)
C21	0.1346(8)	0.023(1)	0.155(1)	0.621(1)	0.014(1)	0.035(1)
C22	0.1825(8)	0.025(1)	0.111(1)	0.656(1)	−0.016(1)	−0.019(1)
C23	0.186(1)	−0.002(1)	0.032(1)	0.654(1)	0.000(1)	−0.106(2)
C24	0.139(1)	−0.034(1)	−0.002(1)	0.620(1)	0.053(1)	−0.134(2)
C25	0.089(1)	−0.037(1)	0.038(1)	0.584(1)	0.084(1)	−0.084(2)
C26	0.0855(8)	−0.007(1)	0.117(1)	0.584(1)	0.067(1)	0.001(2)
C32	0.1003(9)	−0.011(1)	0.317(1)	0.6925(9)	−0.036(1)	0.163(1)
C32	0.104(1)	−0.073(1)	0.287(2)	0.704(1)	−0.106(1)	0.168(2)
C33	0.086(1)	−0.127(1)	0.340(2)	0.764(1)	−0.124(2)	0.187(2)
C34	0.066(1)	−0.116(1)	0.417(2)	0.804(1)	−0.079(2)	0.193(2)
C35	0.064(1)	−0.050(1)	0.446(1)	0.795(1)	−0.012(1)	0.186(2)
C36	0.0803(9)	0.001(1)	0.397(1)	0.735(1)	0.009(1)	0.173(1)
C41	0.0751(8)	0.190(1)	0.028(1)	0.714(1)	0.078(1)	0.370(1)
C42	0.0334(8)	0.234(1)	−0.002(1)	0.737(1)	0.122(1)	0.321(2)
C43	−0.0012(9)	0.216(1)	−0.074(1)	0.795(1)	0.142(1)	0.337(2)
C44	0.008(1)	0.155(1)	−0.114(1)	0.824(1)	0.118(1)	0.409(2)
C45	0.0520(8)	0.113(1)	−0.093(1)	0.800(1)	0.076(1)	0.462(2)
C46	0.0848(8)	0.129(1)	−0.011(1)	0.743(1)	0.055(1)	0.446(1)
C51	0.1093(8)	0.298(1)	0.131(1)	0.613(1)	0.103(1)	0.446(1)
C52	0.0709(8)	0.333(1)	0.179(1)	0.620(1)	0.173(1)	0.439(2)
C53	0.067(1)	0.404(1)	0.176(1)	0.606(2)	0.214(2)	0.509(2)
C54	0.107(1)	0.436(1)	0.129(1)	0.580(1)	0.181(2)	0.574(2)
C55	0.144(1)	0.404(1)	0.083(2)	0.576(1)	0.115(2)	0.584(2)
C56	0.146(1)	0.335(1)	0.081(1)	0.590(1)	0.074(1)	0.517(2)
C61	0.1866(8)	0.191(1)	0.113(1)	0.633(1)	−0.030(1)	0.386(1)
C62	0.2080(9)	0.0184(1)	0.036(1)	0.584(1)	−0.057(1)	0.414(2)
C63	0.266(1)	0.177(1)	0.034(1)	0.583(1)	−0.0126(1)	0.431(2)
C64	0.301(1)	0.176(1)	0.103(1)	0.628(1)	−0.165(1)	0.420(2)
C65	0.289(1)	0.184(1)	0.182(1)	0.677(1)	−0.140(1)	0.391(2)
C66	0.2224(9)	0.194(1)	0.183(1)	0.682(1)	−0.072(1)	0.373(1)

Acknowledgments

Acknowledgement is made to the Donors of the Petroleum Research Fund, administered by the American Chemical Society, for the partial support of this research. We also thank the New Zealand Universities Grants Committee for grants towards instrumental facilities.

References

1 E.O. Fischer, J. Chen and K.J. Scherzer, J. Organomet. Chem., 253 (1983) 231.
2 G.R. Clark, C.E.L. Headford, K. Marsden and W.R. Roper, J. Organomet. Chem., 231 (1982) 335.
3 W.R. Roper, J. Organomet. Chem., 300 (1986) 167.
4 K.R. Grundy and W.R. Roper, J. Organomet. Chem., 216 (1981) 255.
5 K.R. Grundy and W.R. Roper, J. Organomet. Chem., 113 (1976) C45.
6 M. Herberhold, A.F. Hill, G.R. Clark, C.E.F. Rickard, W.R. Roper, A.H. Wright, Organometallics, 8 (1989) 2483; M. Herberhold, A.F. Hill, N. McAuley, W.R. Roper, J. Organomet. Chem., 310 (1986) 95.
7 R. Kuwae, K. Kawakami and T. Tanaka, Inorg. Chim. Acta, 22 (1977) 39.
8 C.E.F. Rickard, W.R. Roper, L.J. Wright and L. Young, J. Organomet. Chem., 364 (1989) 391.
9 A.K. Burrell, Ph.D. Thesis, University of Auckland, 1989.
10 R.L. Hunt, D.M. Roundhill and G. Wilkinson, J. Chem. Soc. (A), (1967) 982.
11 P.B. Hitchcock, M. McPartlin and R. Mason, J. Chem. Soc., Chem. Commun., (1967) 1367.
12 J.A. Evans and D.R. Russell, J. Chem. Soc., Chem. Commun., (1971) 197.
13 R.R. Burch, R.L. Harlow and S.D. Ittel, Organometallics, 6 (1987) 982.
14 L.J. Guggenberger and R. Cramer, J. Am. Chem. Soc., 94 (1972) 3779.
15 D.R. Russell and P.A. Tucker, J. Chem. Soc., Dalton Trans., (1975) 1752.
16 M. Green, J.A.K. Howard, J.L. Spencer and F.G.A. Stone, J. Chem. Soc., Chem. Commun., (1975) 449.
17 J.A.K. Howard, P. Mitrprachachon and A. Roy, J. Organomet. Chem., 235 (1982) 375.
18 M. Cooke, M. Green and T.A. Kuc, J. Chem. Soc. (A), (1971) 1200.
19 G. Agnès, J.C. Bart, C. Santini and K.A. Woode, J. Am. Chem. Soc., 104 (1982) 5254.
20 K.A. Woode, J.C. Bart, M. Calcaterra and G. Agnès, Organometallics, 2 (1983) 627.
21 A. Mayr, A.M. Dorries and G.A. McDermott, J. Am. Chem. Soc., 107 (1985) 7775.
22 Y.T. Struchkov, V.G. Andrianov, V.N. Setkina, N.K. Baranetskaya, V.I. Losikina and D.N. Kursanov, J. Organomet. Chem., 182 (1979) 213.
23 G. Hunter, T.J.R. Weakly, K. Mislow and M.G. Wong, J. Chem. Soc., Dalton Trans., (1986) 577.
24 J.R. Morrow, T.L. Tonker and J.L. Templeton, J. Am. Chem. Soc., 107 (1985) 6956.
25 J. Clemens, M. Green and F.G.A. Stone, J. Chem. Soc., Dalton Trans., (1973) 375.
26 B.E. Cavit, K.R. Grundy and W.R. Roper, J. Chem. Soc., Chem. Commun., (1972) 60.
27 T.J. Collins, K.R. Grundy and W.R. Roper, J. Organomet. Chem., 231, (1982) 161.
28 A.F. Hill, W.R. Roper, J.M. Waters, and A.H. Wright, J. Am. Chem. Soc., 105 (1983) 5939.
29 E.E. Lewis and M.A. Naylor, J. Am. Chem. Soc., 69 (1947) 1968.
30 A.C. North, D.C. Phillips and F.S. Mathews, Acta, Crystallogr., Sect. A, 24 (1968) 351.